Communication

Compact CRLH Leaky-Wave Antenna Using TE_{20}-Mode Substrate-Integrated Waveguide for Broad Space Radiation Coverage

Anirban Sarkar, Abhishek Sharma, Animesh Biswas, and M. Jaleel Akhtar

***Abstract*— In this communication, a composite right-/left-handed (CRLH) based four-quadrant dual-beam scanning leaky-wave antenna is proposed and demonstrated using substrate-integrated waveguide (SIW) technology. The simultaneous use of dual-radiating sections of the TE_{20}-mode SIW makes the structure quite compact with the enhancement in overall gain as compared to the TE_{10}-mode SIW. In addition to this, the incorporation of interdigital slots on the top as well as the bottom plates of the waveguide enables the feature of CRLH media, resulting in full-space beam scanning. Based on the orientation of the electric field on the guiding structure, the top and bottom slots are orthogonally placed to each other. The unit cell characteristics and space harmonics are thoroughly investigated using the dispersion and Bloch impedance analysis. By tactfully tuning the design parameters, the balanced condition is obtained at the broadside frequency of 11.5 GHz. The radiated dual beam covers a four-quadrant scanning range of 248°, having the beam steering from −75° to 49° for both top and bottom halves of the space. The proposed antenna operates within 10–12.8 GHz with a peak gain of 18 dBi. The designed antenna is finally fabricated and tested, where the simulated responses are found in good agreement with the corresponding measured data.**

***Index Terms*— Composite right/left handed (CRLH), leaky-wave antenna (LWA), substrate-integrated waveguide (SIW).**

I. Introduction

Leaky-wave antennas (LWAs) fall under the general category of traveling-wave antennas, where the electromagnetic (EM) wave travels along the structure with decaying power [1], [2]. For such types of structure, the power corresponding to the leaky mode keeps decaying as the radiation occurs continuously along its length, thereby exhibiting a traveling wave type of radiator operating over a specified frequency band. Due to various attractive features such as the frequency beam scanning, simple configuration, narrow beamwidth, and so on, the LWAs are widely used in many applications such as the angle diversity, surveillance systems, and so on. It is to be noted that most of the conventional antennas such as patch and dipole usually have narrow bandwidth due to their resonant nature, involve complex matching network design for array applications, and hence, are not usually suitable for the aforementioned applications. Although some LWAs exhibiting wider operating bandwidth have been reported in the past [3]–[5], the reported configurations radiate only along the broadside direction without providing the beam scanning capability. Moreover, it is essentially required for such types of LWAs to possess higher directional properties over a wide operating bandwidth in addition to a larger beam scanning range. Hence, the dual-beam LWAs appear to be quite appropriate for such types of applications. In literature, few studies have been conducted to realize dual-beam LWAs, showing structural benefits for specified applications. However, they usually either suffer from the limited scanning range or the lower gain [4], [6]–[8].

Over the recent years, the substrate-integrated waveguide (SIW) technology has widely been used to implement LWAs possessing characteristics such as ease of integration, high power handling, good isolation, lightweight, and low cost [9]. However, most of the earlier proposed SIW-based LWAs [10]–[13] are either uniform or quasiuniform types suffering from limited scanning range within the forward region. The use of periodic LWAs (PLWAs) appears to be quite appropriate, where the periodic perturbations along the length of the nonradiating geometry may be introduced to facilitate beam steering from backward to forward direction [14]. Over the past few years, a considerable effort has been made to design SIW-based composite right-/left-handed (CRLH) LWAs to facilitate continuous backward to forward beam scanning through broadside [15]–[21]. However, most of the reported designs either have a larger electrical size or possess a lesser beam scanning range with the typical maximum radiation efficiency of 80%. Recently, the higher-order mode of SIW [22] has been utilized for antenna designs due to its capability to hold larger radiating sections [23]–[25], with a single feed as compared to fundamental TE_{10}-mode SIWs. The usage of higher-order mode SIW basically results in compact configuration due to the utilization of multiple sections for radiation without requiring new physical interconnection. In addition, due to the asymmetry of the radiated fields at both the sides of the SIW transmission line, the equivalent magnetic currents are added in phase at the center of the antenna which causes directivity improvement. In [24], a TE_{20}-mode SIW structure has been utilized to design the high gain dual-beam LWA; however, the antenna scans only two quadrants with limited scanning range. In [5], a double-sided LWA has been proposed which shows improved radiation properties and higher directivity. However, it also exhibits a very limited scanning range. It can be inferred from the aforementioned work that it is quite challenging to design a dual-beam LWA with high gain over the full operating frequency band while maintaining an adequate scanning range, design simplicity, and compactness.

In this communication, the above issues are tackled by designing a novel and simple dual-beam CRLH LWA capable of scanning all the four quadrants from backward to forward through broadside. The proposed antenna is based on the TE_{20}-mode SIW, where the CRLH property is achieved by placing interdigital capacitive slots (IDCs) on the top and bottom metallic wall of TE_{20}-mode SIW. The IDC is placed in accordance with the fields of TE_{20} mode which provides two simultaneously scanning beams. The performance of the proposed antenna is optimized using HFSS and validated through experiments. The proposed antenna is $5.7\lambda_0$ long and scans from −75° to +49° for each of the upper and lower halves of the visible space by varying the frequency from 10 to 12.8 GHz. As a whole, the dual-beam coverage of 248° is achieved using the proposed CRLH LWA along with high gain and compact geometry.

Manuscript received May 29, 2019; revised February 27, 2020; accepted February 29, 2020. Date of publication March 13, 2020; date of current version October 6, 2020. *(Corresponding author: Anirban Sarkar.)*

The authors are with the Department of Electrical Engineering, IIT Kanpur, Kanpur 208016, India (e-mail: anirban.skr227@gmail.com).

Color versions of one or more of the figures in this communication are available online at http://ieeexplore.ieee.org.

Digital Object Identifier 10.1109/TAP.2020.2979229

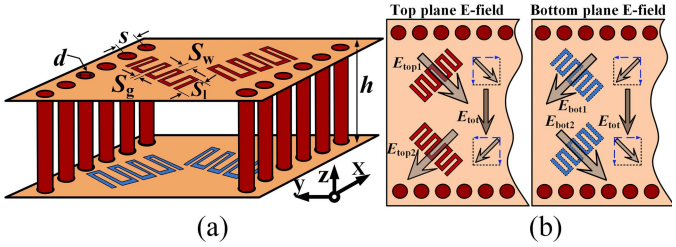

Fig. 1. (a) Layout of proposed TE_{20}-based SIW CRLH unit cell. (b) Orientation of electric field vector on the slots of the unit cell.

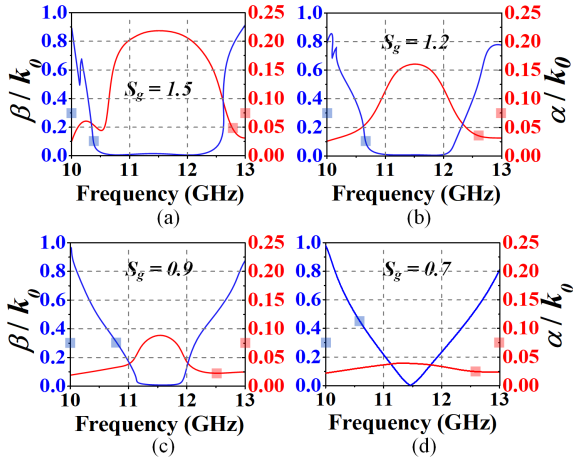

Fig. 2. Variation of physical parameter S_g of the unit cell to achieve the balance condition. (a) S_g = 1.5 mm. (b) S_g = 1.2 mm. (c) S_g = 0.9 mm. (d) S_g = 0.7 mm.

In this communication, Section II includes the design methodology of CRLH unit cell which comprises the TE_{20}-mode SIW incorporated by the quad of IDCs. The analysis of dispersion behavior and Bloch impedance using the full-wave simulation and the equivalent circuit approach are also provided in this section. In Section III, the design principle of the proposed LWA is explained along with the excitation mechanism by microstrip–slotline–TE_{20}-mode SIW transition. The achieved responses from both the simulation and the measurement along with comparative study with the previous works are described in Section IV. Finally, a conclusion is drawn based on the entire analysis and design suitability to meet the desired requirement.

II. TE_{20}-Mode SIW-Based CRLH Unit Cell Design Methodology

Initially, a TE_{20}-mode SIW transmission line is designed, where the electric field has the same amplitude but 180° out of phase along the symmetrical plane of the SIW [24]. Thereafter, to implement a dual-beam full-space scanning LWA, a CRLH structure is realized using tilted IDCs etched on the upper and lower metallic walls of the SIW. These radiating slots are placed in accordance with the electric field distribution of TE_{20} mode [refer Fig. 1(a) and (b)] and made center symmetric by placing them at an angle of ±45° with respect to the magnetic walls. It is worth mentioning that balancing the CRLH unit cell is critically important to avoid the issue of open stopband along the broadside direction that predominantly restricts radiation. To achieve a balanced unit cell, the elimination of the stopband can be performed by tuning the geometrical parameters such as S_g, S_w, and S_l. For example, the suppression of open stopband based on optimizing the parameter S_g is shown in Fig. 2, where the stopband is completely eliminated for $S_g = 0.7$ mm. Basically, the interdigital

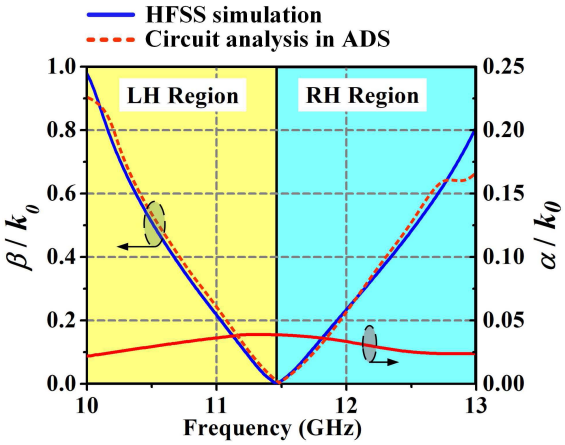

Fig. 3. Dispersion diagram of the proposed unit cell.

slots on the top and bottom layers can be modeled as series capacitors (or left-handed capacitance, C_L), and the metallic vias are responsible for the shunt inductance (or left-handed inductance, L_L). The upper and lower metallic walls form a series inductance (or right-handed inductance, L_R) and distributed shunt capacitance (or right-handed capacitance, C_R). The electric field vector orientation on the top as well as the bottom plane is shown in Fig. 1(b). The balanced condition occurs when the left- and right-handed contributions exactly balance each other at a given frequency, leading to the condition

$$\frac{L_R}{L_L} = \frac{C_R}{C_L}. \tag{1}$$

The unit cell described above is simulated using the full-wave EM solver HFSS with periodic boundary condition, and S-parameters are extracted to study the dispersion and Bloch impedance characteristics. The dispersion curve of the proposed balanced unit cell is shown in Fig. 3, which is obtained by employing the analysis given in [20]. The balanced condition for the proposed design is obtained at 11.5 GHz, by controlling the LH and RH media near the balanced point as shown in Fig. 3. In addition, the normalized attenuation constant ($|\alpha|/k_0$) exhibits smooth behavior with frequencies, indicating that the radiated beam will not be degraded with frequency variation. Furthermore, the circuit analysis is performed using Advanced Design System (ADS), where dispersion characteristic is obtained through gradient optimization. For the circuit analysis, four IDCs (two slots on each of the top and bottom planes) are considered as four LC-tank circuits. The change in circuit element values from the initial prediction gives an insight into the direction of required change in physical parameters of the unit cell in simulation to achieve a balanced condition. Since the unit cell consists of four IDCs (two IDCs with 180° out of phase in the top metallic plane and two IDCs with 180° out of phase in bottom metallic plane), the overall L_L and C_L include the combined effect of all left-handed contribution of inductance and capacitance. The optimized circuit parameters are: L_L = 1.18 nH, C_L = 0.9 pF, L_R = 1.45 nH, and C_R = 1.1 pF. The circuit analysis results obtained using ADS agrees well with the full-wave simulation as shown in Fig. 3. In order to estimate β/k_0 and α/k_0 more appropriately, the finite structure having 11 unit cells is considered. Fig. 4(a) and (b) shows the dispersion characteristics of full structure for both the unbalanced and balanced cases, respectively. It is clear from the figure that the unbalanced structure shows the presence of sharp stopband at broadside frequency region, whereas a good matching is obtained for the balanced case with complete suppression of stopband.

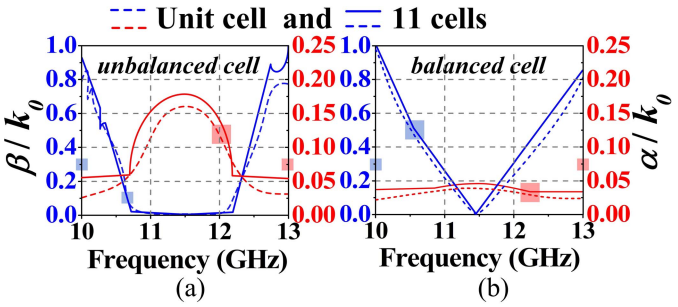

Fig. 4. Characteristics of dispersion curve with the variation of a number of cells for (a) unbalanced and (b) balanced structure.

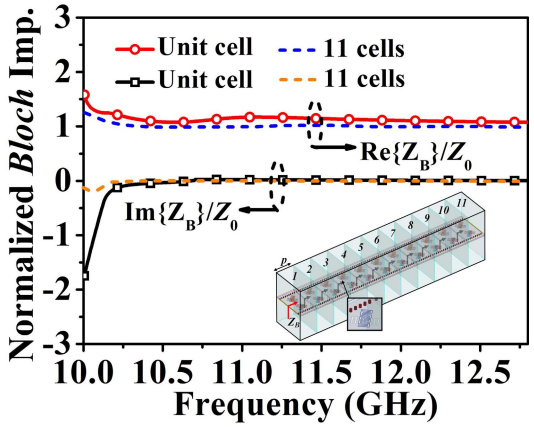

Fig. 5. Variation of Bloch impedance with frequencies with increment of cell numbers.

Next, the Bloch impedance is determined using the following expression (2) [20], [26]. The Bloch analysis here is carried out for both unit cell and finite structure having 11 unit cells [27]. The periodic boundary condition is used in the former case, whereas in the latter case, the radiation boundary condition is utilized

$$Z_B = \pm Z_0 \sqrt{\frac{(1+S_{11})^2 - S_{21}^2}{(1-S_{11})^2 - S_{21}^2}}. \tag{2}$$

Moreover, to simplify the analysis, the radiation resistance is neglected. The normalized Bloch impedance (Z_B/Z_0) for both unit cell and finite structure is shown in Fig. 5, indicating the impedance matching throughout the frequency band. It is to be noted that this impedance matching is improved in the case of 11 unit cells, where $\mathrm{Re}\{Z_B/Z_0\} \sim 1$ and $\mathrm{Im}\{Z_B/Z_0\} \sim 0$ over the desired frequency band. This TE_{20}-mode SIW-based effective CRLH unit cell is utilized to design the proposed antenna structure as described in Section III.

III. LWA Design

The fast-wave characteristic of the TE_{20}-mode SIW transmission line facilitates the design of LWA with fundamental space harmonic, i.e., $n = 0$. However, it can only provide a limited scanning range in the forward quadrant. To facilitate the beam scanning from backward to forward along with broadside, the SIW is periodically loaded with the proposed CRLH unit cell having periodicity p along the x-axis of the structure. To demonstrate the effectiveness of the concept, a finite lossless structure having 11 cells is designed and optimized through full-wave simulation. The layout of the proposed antenna is shown in Fig. 6(a). It can be observed from this figure that the microstrip–slotline–SIW transitions are used at the input and output

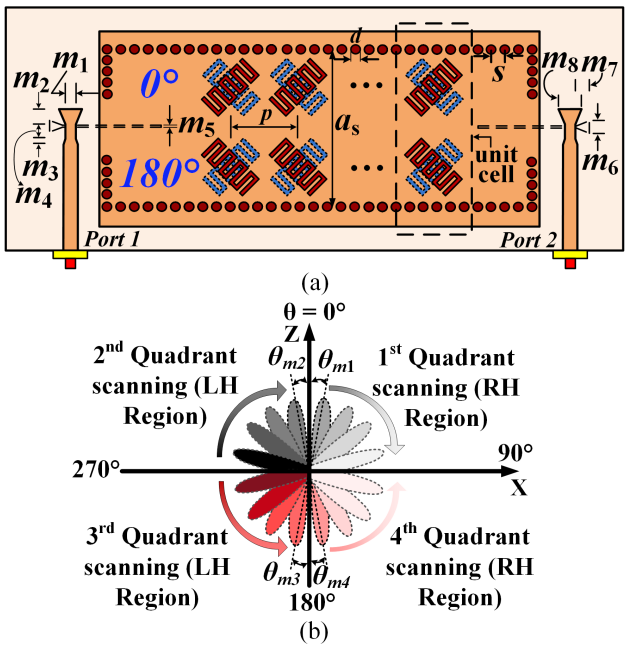

Fig. 6. (a) Layout of the proposed antenna. (b) Quadrant-wise beam scanning layout.

ports of TE_{20}-mode structure. Basically, the two-step transitions have been exploited here to realize the wideband TE_{20}-mode excitation. It is observed that one transition is acting as a mode converter from slotline to the higher-order mode of SIW, where the horizontally polarized electric field of the slotline is converted to the vertically polarized field of the SIW. Since the amplitude maximum exists at the center of the half-wavelength resonator (quarter wavelength away from the shorted termination), a portion of slotline having a length of $\lambda_g/2$ is extended inside the SIW to achieve high coupling between slotline and SIW. By using slotlines, the electric field with equal magnitude but reversed phase is formed along the symmetrical plane of the SIW [24] (field plot is not shown here for brevity). For the better impedance matching, few vias are placed at the edge of SIW section. In the present design, the dimensional parameter m_5 is kept as minimum as possible according to the minimum fabrication precision for reducing any significant radiation losses during slotline to SIW-mode conversion. Another stage of transition is input microstrip line to grounded slotline, where the length of the triangular microstrip stub m_2 is set to be a $\lambda_g/4$ to ensure a high coupling between the microstrip line and slotline resonator. For fine tuning, all the other design parameters are optimized accordingly using full-wave simulator HFSS. A prototype is built on Rogers RT/duroid 5880 substrate of thickness 0.787 mm having $\epsilon_r = 2.2$ and $\tan\delta = 0.0009$. It is worth mentioning here that the excitation of the fundamental TE_{10} mode is effectively suppressed and made localized by utilizing the specified feeding mechanism. Hence, only TE_{20} mode is dominant throughout the structure in the present situation. The periodicity p of the slots is maintained by taking care of the homogeneity condition, i.e., $p \ll \lambda_0/4$. The scanning angle of the proposed antenna depends on nth spatial harmonic β_n and the free-space wavenumber k_0. The antenna is working in fast-wave region, where the range of β_n is $-k_0 < \beta_n < k_0$ having the scanning capability from backward ($\theta = -90°$) to forward quadrant ($\theta = 90°$) including broadside ($\theta = 0°$). The antenna is operating at the fundamental space harmonic, i.e., $n = 0$. The direction of maximum radiation from z-axis and 3 dB beamwidth of the LWA with a radiator length of L_A can be determined from [28].

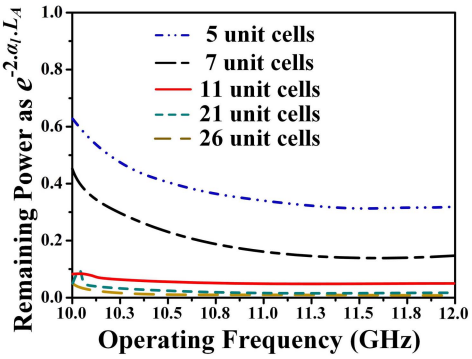

Fig. 7. Variation of radiator length and its effect on remaining power at *Port 2*.

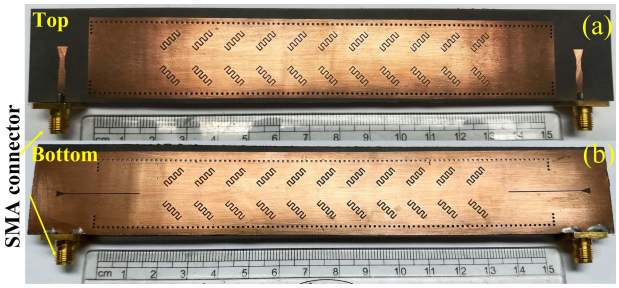

Fig. 8. (a) Top view and (b) bottom view of the fabricated prototype of the proposed antenna.

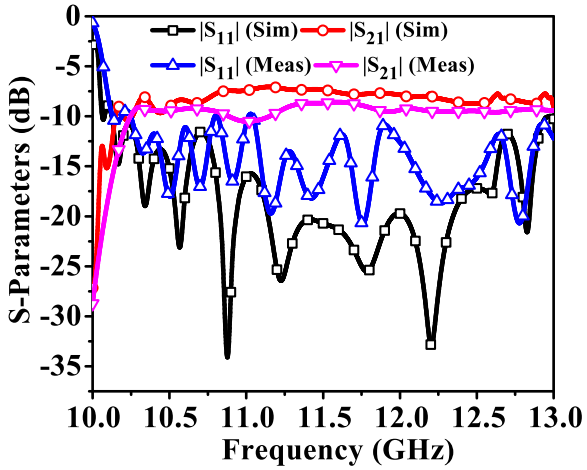

Fig. 9. Comparison of simulated and measured S-parameter responses of the proposed antenna.

The radiator length L_A is chosen such that almost 90%–95% power radiates from the structure, whereas remaining 5%–10% power may reach at the *Port 2* of the antenna, which actually provides no significant reflection mismatch at the other end [2]. The variation of the radiator length and the corresponding remaining power at *Port 2* are shown in Fig. 7. It is clear that the radiated power from the structure increases with the increment of the number of cells and is optimum for $L_A = 5.7\lambda_0$, consisting of 11 unit cells, where the radiated power is almost 95%. For the proposed structure, the radiation from the top slots scans from second to first quadrant, whereas the bottom slots scan from third to fourth quadrant. Thus, these simultaneous dual-radiated beams scan all the four quadrants with frequency variation as shown in Fig. 6(b).

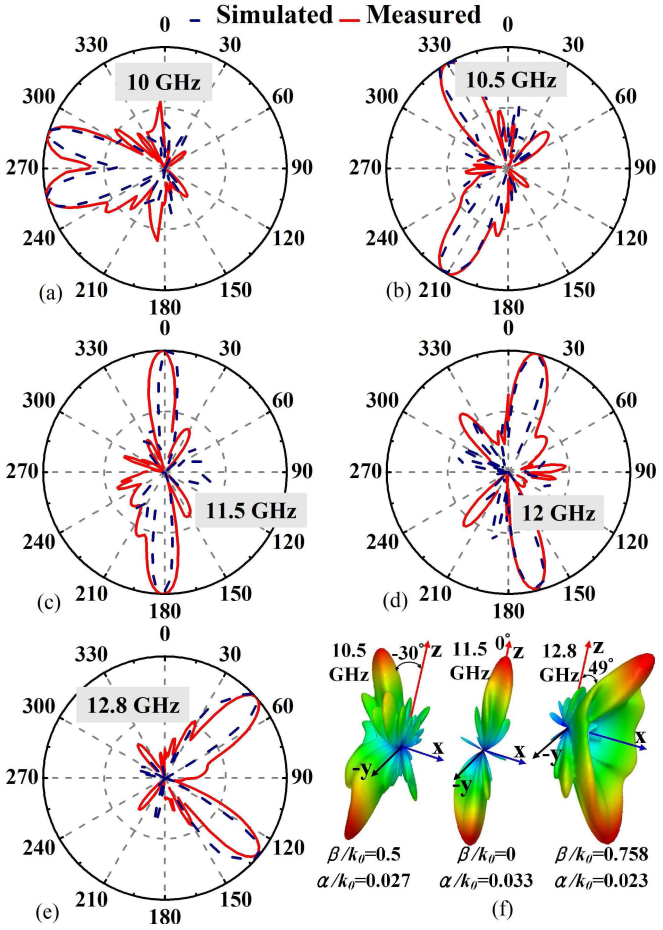

Fig. 10. (a)–(e) xz plane radiation patterns of the proposed antenna at different frequencies and (f) 3-D radiation patterns of the proposed antenna at 10.5, 11.5, and 12.8 GHz.

IV. Results and Discussion

To validate the proposed concept experimentally, the designed antenna is fabricated using the PCB technology for testing as shown in Fig. 8. The final optimized dimensions are $a_s = 22.3$ mm, $d = 0.8$ mm, $s = 1.6$ mm, $S_g = 0.7$ mm, $S_l = 2$ mm, $S_w = 1.3$ mm, $p = 10$ mm, $m_1 = 1.6$ mm, $m_2 = 3.4$ mm, $m_3 = 1.16$ mm, $m_4 = 3.3$ mm, $m_5 = 0.2$ mm, $m_6 = 2$ mm, $m_7 = 3$ mm, and $m_8 = 3.5$ mm. The prototype is only $5.7\lambda_0$ long having 11 unit cells. The simulated and measured S-parameter responses of the proposed LWA are in good agreement as shown in Fig. 9. The proposed antenna operates from 10 to 12.8 GHz, having -10 dB impedance bandwidth of 24.56%. The simulated and measured normalized radiation patterns in yz plane are compared and shown in Fig. 10(a)–(e). From the figure, it is clear that the proposed antenna covers a scanning range of $\pm 124°$ for each of the top and bottom planes with the frequency variation from 10 to 12.8 GHz. The radiated dual beam scans all the four quadrants with the frequency variation from 10 to 12.8 GHz. The beam on the top plane scans the first and second quadrants, whereas the beam at the bottom plane scans simultaneously the third and fourth quadrants. Thus, the proposed dual-beam LWA covers all the four quadrants with the overall beam coverage of 248°. The broadside ($\pm z$-direction) radiation is obtained at 11.5 GHz, and the measured sidelobe level is less than -10 dB throughout the working band. Fig. 10(f) shows the 3-D radiation pattern for three different frequencies with corresponding values of normalized β, α, and the beam pointing angle. The measured peak gain (G_P) of the

TABLE I

PERFORMANCE COMPARISON OF PROPOSED STRUCTURE WITH THE CLOSELY RELATED CRLH AND TE_{20}-MODE SIW-BASED LWA

Reference	Type	Freq. (Bandwidth)	Length	$\Delta\theta$ (Scanning range)	G_P (dBi)	η_{f_0}
[4]	Only dual-beam	6.92-8.75 GHz(23%)	$5.87\lambda_0$	37° (75° to 38°)	12.7 (9.5 to 12.7)	-
[5]	TE_{20} SIW based	13.5-16.5 GHz(20%)	$6.47\lambda_0$	43°	15.1 (14.1-15.1)	90%
[6]	Only dual-beam	11.58-12.5 GHz(7.64%)	$3.9\lambda_0$	20°	10	-
[15]	CRLH with IDC	8.6-12.8 GHz (39.25%)	$7\lambda_0$	130° (-70° to +60°)	10.8 (4.4-10.8)	78%
[16]	CRLH with IDC	7.5-10 GHz (25.57%)	$5.6\lambda_0$	80° (-30° to +40°)	12 (9.72-12)	80%
[17]	CRLH with IDC	7.4-13.5 GHz(54%)	$6.2\lambda_0$	140°(-70° to +70°	12.01 (7.48-12.01)	NA
[18]	CRLH with IDC	4.2-4.85 GHz(14.36%)	$2.42\lambda_0$	51° (-25° to +26°)	2.5 (0-2.5)	NA
[19]	CRLH with IDC	7.15-10.35 GHz(36.57%)	$5.6\lambda_0$	103° (-19° to +84°)	8.95 (0-8.95)	69%
[24]	TE_{20} SIW+dual-beam	9.6-11.2 GHz(15.38%)	$7\lambda_0$	132° (top:66°+bottom:66°)	14 (12.5-14)	97%
This work	**CRLH+TE_{20} SIW+dual beam**	**10-12.8 GHz(24.56%)**	**$5.7\lambda_0$**	**248° (top:124°+bottom:124°)**	**18 (16.2-18)**	**98%**

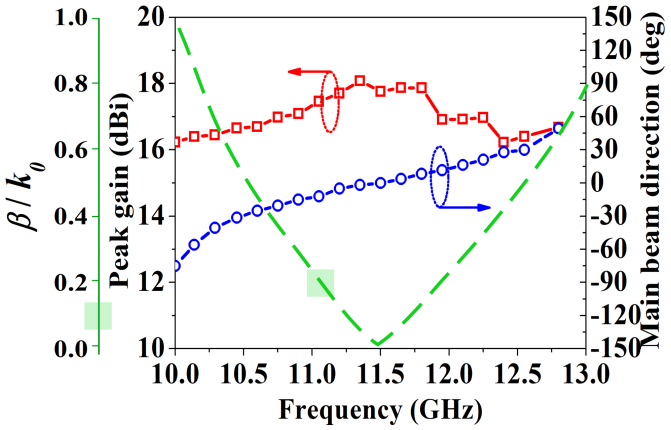

Fig. 11. Variation of peak gain and direction of radiated main beam with the variation of frequencies.

proposed antenna ranges from 16.2 to 18 dBi across the operating band as shown in Fig. 11. It is worth mentioning here that since the radiated power criteria are already maintained for the proposed design, therefore any further increase in the number of unit cell causes a negligible impact on gain enhancement. As a matter of fact, the increase of radiator length from $5.7\lambda_0$ to $11\lambda_0$ (almost doubling the radiator length) creates an overall gain increment of only 1.5 dBi. The variation of main beam direction with frequency is also shown in Fig. 11 (blue curve) along with the corresponding simulated phase constants (green dashed line), which proves the validity of the antenna radiated beam direction.

A detailed comparison of the proposed work with other reported works is shown in Table I. In comparison to the earlier work proposed such as in [4], [16], and [19], the present work is advantageous in terms of its much larger radiation coverage, high gain, and radiation efficiency having comparable radiator lengths and bandwidths. Although the works reported in [5] and [24] have used TE_{20}-mode SIW to design LWA with comparable efficiency and operating bandwidth, the proposed LWA design achieves a higher scanning range along with the compact size. Thus, the work proposed herein possesses the merits of having wider scanning range, higher gain, and larger radiation efficiency along with the much compact geometry.

V. CONCLUSION

The design and implementation of a TE_{20}-mode SIW-based four-quadrant beam scanning CRLH LWA has been successfully demonstrated. The CRLH media have been realized by placing tilted interdigital slots on the top and bottom magnetic metallic walls of the TE_{20}-mode SIW. The proposed antenna is compact having an overall dimension of $5.7\lambda_0 \times 1.3\lambda_0 \times 0.03\lambda_0$ and has achieved the beam scanning range of $-75°$ to $49°$ for each of the upper and lower halves of the visible space, providing a total of 248° scan in all the four quadrants. Across the operating band of 10–12.8 GHz, the variation of peak gain is from 16.2 to 18 dBi. The performance of the proposed LWA prototype shows considerable advantages over the recently proposed SIW-CRLH-based dual-beam LWAs in terms of scanning range, size, gain, and radiation efficiency. The proposed LWA could be a potential candidate for automotive radar systems, collision warning radar systems, wireless applications, vehicular communication, and so on.

REFERENCES

[1] D. R. Jackson, C. Caloz, and T. Itoh, "Leaky-wave antennas," *Proc. IEEE*, vol. 100, no. 7, pp. 2194–2206, Jul. 2012.
[2] D. R. Jackson and A. A. Oliner, "Leaky-wave antennas," in *Modern Antenna Handbook*, C. A. Balanis, Ed. Hoboken, NJ, USA: Wiley, 2008.
[3] D. Comite *et al.*, "Analysis and design of a compact leaky-wave antenna for wide-band broadside radiation," *Sci. Rep.*, vol. 8, no. 1, pp. 1–14, Dec. 2018.
[4] D. K. Karmokar, K. P. Esselle, and T. S. Bird, "Wideband microstrip leaky-wave antennas with two symmetrical side beams for simultaneous dual-beam scanning," *IEEE Trans. Antennas Propag.*, vol. 64, no. 4, pp. 1262–1269, Apr. 2016.
[5] A. J. Martinez-Ros, M. Bozzi, and M. Pasian, "Double-sided SIW leaky-wave antenna with increased directivity in the *E*-plane," *IEEE Trans. Antennas Propag.*, vol. 66, no. 6, pp. 3130–3135, Jun. 2018.
[6] C.-C. Hu, C. F. Jsu, and J.-J. Wu, "An aperture-coupled linear microstrip leaky-wave antenna array with two-dimensional dual-beam scanning capability," *IEEE Trans. Antennas Propag.*, vol. 48, no. 6, pp. 909–913, Jun. 2000.
[7] Z. L. Ma and L. J. Jiang, "One-dimensional triple periodic dual-beam microstrip leaky-wave antenna," *IEEE Antennas Wireless Propag. Lett.*, vol. 14, pp. 390–393, 2015.
[8] A. Sarkar, S. Mukherjee, A. Sharma, A. Biswas, and M. J. Akhtar, "SIW-based quad-beam leaky-wave antenna with polarization diversity for four-quadrant scanning applications," *IEEE Trans. Antennas Propag.*, vol. 66, no. 8, pp. 3918–3925, Aug. 2018.
[9] D. Deslandes and K. Wu, "Single-substrate integration technique of planar circuits and waveguide filters," *IEEE Trans. Microw. Theory Techn.*, vol. 51, no. 2, pp. 593–596, Feb. 2003.
[10] Y. J. Cheng, W. Hong, K. Wu, and Y. Fan, "Millimeter-wave substrate integrated waveguide long slot leaky-wave antennas and two-dimensional multibeam applications," *IEEE Trans. Antennas Propag.*, vol. 59, no. 1, pp. 40–47, Jan. 2011.

[11] J. Liu, D. R. Jackson, and Y. Long, "Substrate integrated waveguide (SIW) leaky-wave antenna with transverse slots," *IEEE Trans. Antennas Propag.*, vol. 60, no. 1, pp. 20–29, Jan. 2012.

[12] J. Liu, X. Tang, Y. Li, and Y. Long, "Substrate integrated waveguide leaky-wave antenna with H-shaped slots," *IEEE Trans. Antennas Propag.*, vol. 60, no. 8, pp. 3962–3967, Aug. 2012.

[13] J. Liu, D. R. Jackson, Y. Li, C. Zhang, and Y. Long, "Investigations of SIW leaky-wave antenna for endfire-radiation with narrow beam and sidelobe suppression," *IEEE Trans. Antennas Propag.*, vol. 62, no. 9, pp. 4489–4497, Sep. 2014.

[14] J. T. Williams, P. Baccarelli, S. Paulotto, and D. R. Jackson, "1-D combline leaky-wave antenna with the open-stopband suppressed: Design considerations and comparisons with measurements," *IEEE Trans. Antennas Propag.*, vol. 61, no. 9, pp. 4484–4492, Sep. 2013.

[15] Y. Dong and T. Itoh, "Composite right/left-handed substrate integrated waveguide and half mode substrate integrated waveguide leaky-wave structures," *IEEE Trans. Antennas Propag.*, vol. 59, no. 3, pp. 767–775, Mar. 2011.

[16] Y. Dong and T. Itoh, "Substrate integrated composite right-/left-handed leaky-wave structure for polarization-flexible antenna application," *IEEE Trans. Antennas Propag.*, vol. 60, no. 2, pp. 760–771, Feb. 2012.

[17] A. P. Saghati, M. M. Mirsalehi, and M. H. Neshati, "A HMSIW circularly polarized leaky-wave antenna with backward, broadside, and forward radiation," *IEEE Antennas Wireless Propag. Lett.*, vol. 13, pp. 451–454, 2014.

[18] H. Lee, J. H. Choi, C.-T.-M. Wu, and T. Itoh, "A compact single radiator CRLH-inspired circularly polarized leaky-wave antenna based on substrate-integrated waveguide," *IEEE Trans. Antennas Propag.*, vol. 63, no. 10, pp. 4566–4572, Oct. 2015.

[19] M. M. Sabahi, A. A. Heidari, and M. Movahhedi, "A compact CRLH circularly polarized leaky-wave antenna based on substrate-integrated waveguide," *IEEE Trans. Antennas Propag.*, vol. 66, no. 9, pp. 4407–4414, Sep. 2018.

[20] A. Sarkar, M. Adhikary, A. Sharma, A. Biswas, M. J. Akhtar, and Z. Hu, "Composite right/left-handed based compact and high gain leaky-wave antenna using complementary spiral resonator on HMSIW for ku band applications," *IET Microw., Antennas Propag.*, vol. 12, no. 8, pp. 1310–1315, Jul. 2018.

[21] A. Sarkar, A. Sharma, A. Biswas, and M. J. Akhtar, "EMSIW-based compact high gain wide full space scanning LWA with improved broadside radiation profile," *IEEE Trans. Antennas Propag.*, vol. 67, no. 8, pp. 5652–5657, Aug. 2019.

[22] P. Wu, J. Liu, and Q. Xue, "Wideband excitation technology of TE_{20} mode substrate integrated waveguide (SIW) and its applications," *IEEE Trans. Microw. Theory Techn.*, vol. 63, no. 6, pp. 1863–1874, Jun. 2015.

[23] H. Gharibi and F. H. Kashani, "Design of a compact circularly polarized dual-mode monopulse cavity-backed substrate integrated waveguide antenna," *IEEE Antennas Wireless Propag. Lett.*, vol. 14, pp. 519–522, 2015.

[24] A. Sarkar, A. Sharma, M. Adhikary, A. Biswas, and M. J. Akhtar, "Bi-directional SIW leaky-wave antenna using TE_{20} mode for frequency beam scanning," *Electron. Lett.*, vol. 53, no. 15, pp. 1017–1019, Jul. 2017.

[25] H. Jin, W. Che, K.-S. Chin, W. Yang, and Q. Xue, "Millimeter-wave TE_{20}-mode SIW dual-slot-fed patch antenna array with a compact differential feeding network," *IEEE Trans. Antennas Propag.*, vol. 66, no. 1, pp. 456–461, Jan. 2018.

[26] G. Valerio, S. Paulotto, P. Baccarelli, P. Burghignoli, and A. Galli, "Accurate Bloch analysis of 1-D periodic lines through the simulation of truncated structures," *IEEE Trans. Antennas Propag.*, vol. 59, no. 6, pp. 2188–2195, Jun. 2011.

[27] N. Apaydin, L. Zhang, K. Sertel, and J. L. Volakis, "Experimental validation of frozen modes guided on printed coupled transmission lines," *IEEE Trans. Microw. Theory Techn.*, vol. 60, no. 6, pp. 1513–1519, Jun. 2012.

[28] W. Fuscaldo, D. R. Jackson, and A. Galli, "A general and accurate formula for the beamwidth of 1-D leaky-wave antennas," *IEEE Trans. Antennas Propag.*, vol. 65, no. 4, pp. 1670–1679, Apr. 2017.